Reviewer 2:

This paper is an interesting discussion of the link between aerosols, vapor pressure deficit and evapotranspiration over India. The paper presents some interesting findings: 1) sensible heat is lower under heat wave conditions, 2) latent heat is enhanced under aerosol loading due to diffuse fertilization, and 3) decoupling of the vapor pressure deficit response under high aerosol load. These are very interesting findings, as they turn out to be different than what is common knowledge for regions that do not have the aerosol load of India and provides insights into the coupled behavior of air pollution, vegetation, and weather.

We thank the reviewer for his appreciation of the interesting finding of our study. Our point-to-point response to all the comments are provided below in blue font and the corresponding modification in the revised MS is shown in *italics*.

Major comments:

Q. The finding that the evaporation response to vapor pressure deficit becomes really weak under a high aerosol optical depth is very interesting, but also controversial. The authors demonstrate the opposite findings in a modelling study, which shows that their results might be very important. At the same time: one figure (Fig. 4) does not really convince me. The explanation of it remains rather limited and I think that this finding deserves a far more thorough analysis before this paper can be accepted. Vapor pressure deficit is not the only driver of stomatal resistance, and it would be good to carefuly look into each of them. It would be nice to analyze here a few diurnal cycles into detail. I would like to see the evolution of the evapotranspiration and specific humidity, next to the radiation and the surface temperature.

We do acknowledge that due to the statistical nature of the analysis, it is difficult to draw clear mechanistic conclusions. However, these unprecedented set of observations provide a good platform to analyze and gain insights into role of aerosols on VPD-EF associations that can inform further research and model development.

VPD is not only controlling factor for canopy resistance. The interactions between multiple factors, including available energy, temperature, and VPD, control the canopy resistance. Hence, we have investigated the relationships between other factors that control evapotranspiration, namely available energy and moisture demand (the physical factors) and the aerodynamic resistance (a physiological factor) and canopy resistance during the LAHT and HAHT cases (Fig 4cb-d). We have also checked for statistical significant of these relationships. We find that the canopy resistance is only significantly ($p<0.05$) correlated with VPD, not the other two variables. Additionally, the sensitivity of canopy resistance to changes in VPD is much higher than that for the other two variables. Similarly, increase in air temperature during these periods also show statistically significant positive relationships with canopy resistance, which is consistent with our understanding that plants close their stoma at high ambient temperature (Heerwaarden and Teuling, 2016). These additional panels are now added to Figure 4. Also see them below.

We also analysed the diurnal evolution of micro-meteorological variables such as soil temperature and moisture, specific humidity, incoming solar radiation along with latent heat, GPP and CO_2 fluxex. As heatwave was prevalent during HAHT and LAHT weeks with substantial increases in soil temperature, which resulted in minor decrease in soil moisture across both weeks. Moreover, some variations are seen in the evolution of wind speed during HAHT as it decreased by ~3-4 m/s from 10th April to 15th April, 2017 during HAHT. All other meteorological variables showed negligible weekly trends during HAHT.
Largely, evapotranspiration is expected to vary proportionally with wind speed, if all other factors remain same, however we find that both GPP and latent heat, increase gradually during HAHT, indicating secondary/tertiary impact of wind speed variation on evapotranspiration during this week.

During LAHT, all the meteorological variables also showed negligible temporal trends except specific humidity. The specific humidity decreased from 10thMay to 15th May, 2017, which is similar to the decreasing trend in evapotranspiration. The consistency could be probably because evapotranspiration is a main source of near surface moisture over our site during stagnant heat wave conditions in dry season. Thus, a closer look illustrates that although minor gradients are present in the meteorological variables, they are not dominant factors influencing evapotranspiration variation during the two case studies. Nonetheless, the individual or relative contribution of these meteorological variability and aerosols on the observed coupling deserves further attention in future studies with in depth mechanistic modelling.

Modified text:

Line nos: 355-395

Figure 4 illustrates the variation in midday mean canopy resistance during the LAHT and HAHT week to various physical and physiological factors that control evapotranspiration, namely moisture demand, available energy, air temperature and the aerodynamic resistance. As expected, the canopy resistance is significantly ($p<0.05$) correlated with VPD although clear differences in the slope is present for the two cases. Specifically, the canopy resistance increases steeply from 400 to 1400 s m^{-1} with increase in VPD from 40 to 70 hPa during LAHT case (Figure 4a). However, the canopy resistance increases from 400 to 500 with increase in VPD from 45 to 65 hPa during HAHT case (Figure 4a). Similarly, increase in air temperature during these periods also show statistically significant positive relationships with canopy resistance (Figure 4d). However, during both the weeks, canopy resistance was found to be independent of available energy (Figure 4c) and the aerodynamic resistance (Figure 4d), indicating that the sensitivity of canopy resistance to changes in VPD or T_{air} is significantly greater than that for the other variables.

The LAHT case illustrates the frequently reported behaviour of reduction of canopy conductance under increase in VPD due to partial stomata closure as a physiological stress response (Grossiord et al., 2020). Similar responses are also reported in Napier grasses, the native vegetation over our site (Mwendia et al. 2016). Napier grasses can be anisohydric, i.e. water spending under ample water availability (Cardoso et al., 2015). But their behavior becomes isohydric under high temperature and high water stress (Liang et al., 2017; Mwendia et al. 2014; Purbajanti et al., 2012). During both HAHT and LAHT weeks, the soil moisture is very *low. Hence, the Napier grasses behaves isohydric-ally under high VPD. Interestingly, the comparison of LAHT and HAHT scatter illustrates that canopy conductance is not much affected even under severe VPD rise when aerosol loading also increases in phase. Specifically, the strong gradient of increase in canopy resistance with VPD/ air temperature gets moderated under high aerosol scenario. Thus, under the presence of high aerosols loading, this isohydric response of Napier grass to temperature rise or the physiological stress under VPD increase is decoupled. This can partially explain the aerosol-induced increase in EF (as well as LH and GPP) even under high VPD rise during HAHT.*

Further, meteorological co-variability or any significant differences in weekly pattern of other micro-meteorological variables between HAHT and LAHT cases can also contribute to the corresponding differences in AOD-VPD-EF association. A closer look illustrates that minor gradients are present in the meteorological variables (Figure S2), which can have secondary effects on the VPD-EF associations. Nonetheless, the individual or relative contribution of these meteorological variability and aerosols on the observed coupling remains unknown and deserves further attention in future studies with in depth mechanistic modelling.

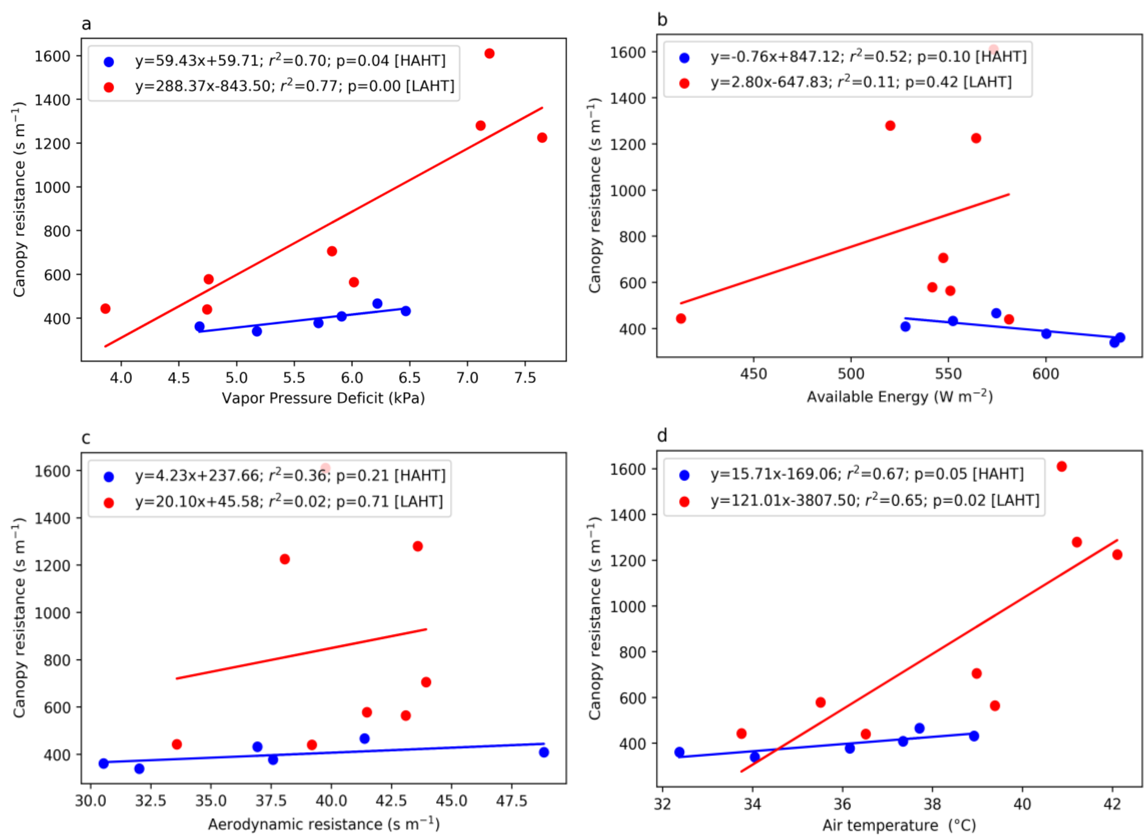

Figure 4: Linear correlation between daily midday average Canopy resistance derived from Penman-Monteith equation with a) observed Vapor Pressure Deficit (VPD); b) Available energy at surface; c) Aerodynamic resistance and d) Air temperature for HAHT and LAHT cases. Modified text

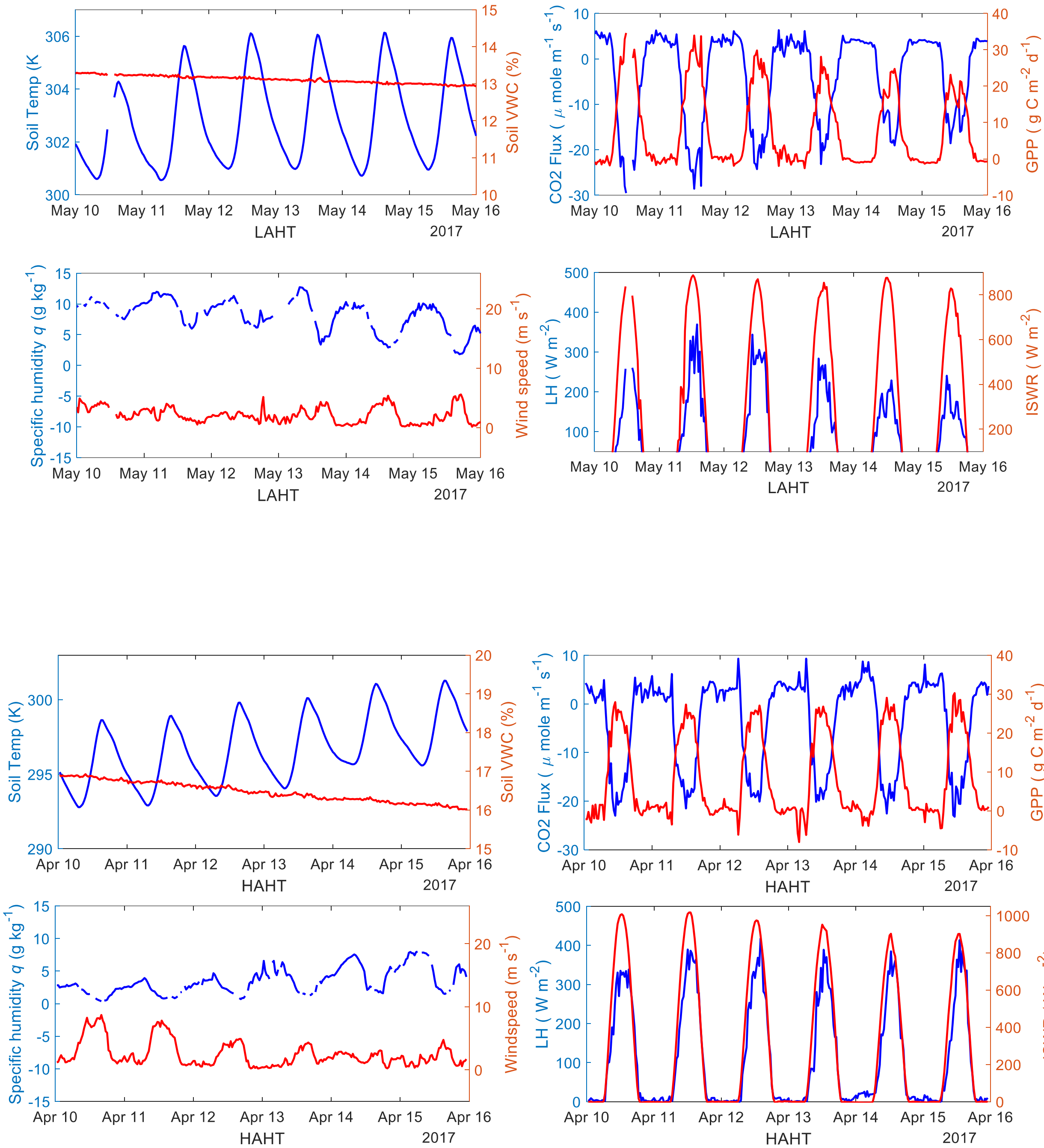

Figure S2: The daily evolution of meteorological variables during LAHT and HAHT weeks.

Q. The inversion of Penman-Monteith that leads to figure 4 is not reproducible. I would like to see this method thorougly described in the paper. Furthermore, I am a little skeptical of using surface temperature here. Please also compute the stomatal resistance using the air temperature as Penman-Monteith does as well.

We have now included the complete methodology in the revised manuscript with the relevant equations. Note that surface temperature is only used to derive aerodynamic resistance using the observed sensible heat flux and near-surface temperature gradient.

Modified text

Line 229

We also calculated the daily midday bulk canopy resistances for both HAHT and LAHT cases by inverting the Penmann-Monteith equation as described below. We used observed values of available energy, VPD, T_{srf} derived from observed LW_{out}, psychrometric constant and slope of vapor pressure curve derived from observed surface pressure and T_{air} respectively, and aerodynamic resistance derived from the observed SH and near-surface temperature gradient.

The aerodynamic resistance to heat transfer (r_a) is calculated from the near-surface temperature gradient and the measured H, given by:

$$r_a = \frac{-\rho Cp\,(Tsrf - Tair)}{H}$$

where T_s is the surface temperature, calculated by inverting the Stefan-Boltzmann law assuming a unit surface emissivity (reasonable for vegetated surfaces), ρ is the air density, and C_p is the specific heat at constant pressure (1.005 x 10^{-3} MJ kg^{-1} °C^{-1}).

Then, the canopy resistance (r_s) is calculated by inverting the Penman-Monteith approximation. Thus:

$$r_s = \frac{\left(\frac{\Delta(Rn - G) + \frac{\rho CpVPD}{r_a}}{LE}\right) - \Delta}{\gamma - 1} r_a$$

where Δ is the slope of the water vapor saturation curve given by:

$$\Delta = \frac{4098[0.6108exp(\frac{17.27T_a}{T_a + 237.3})]}{(T_a + 237.3)^2}$$

and γ is the psychrometric constant, calculated as:

$$\gamma = \frac{C_p P}{\varepsilon\lambda}$$

where P is atmospheric pressure in kPa, λ is the latent heat of vaporization (2.45 MJ kg^{-1}), and ε is the ratio of the molecular weight of water vapour to dry air (0.622).

Minor comments:

* In my view, all acronyms could be replaced by written words in order to make the paper more readable. It does do no harm if the paper is 20 lines longer for that reason.

We have now expanded the abbreviations in most of the new paragraphs in the revised text for ease of readers. Moreover, we have added a table of abbreviations used for ease of the readers.

Appendix A: Table of Abbreviations

Name	***Abrv. used***
Latent heat flux	*LH*
Sensible heat flux	*SH*
Ground heat flux	*GH*
Evaporative Fraction	*EF*
2 m air temperature	T_{air}
vapor pressure deficit	*VPD*
gross primary production	*GPP*
net radiation	*NR*
aerosol direct radiative effect	*ADRE*
aerosol diffuse radiation fertilization effect	*ADFE*
diffuse radiation	$diffuse_{frac}$
Santa Barbara discrete ordinates radiative transfer Atmospheric Radiative Transfer Model	*SBDART*
AErosol RObotic NETwork	*AERONET*
Volumetric soil water content	*VWC*
surface temperature	T_{srf}
relative humidity	*RH*
Aerosol Optical Depth	*AOD*
Single Scattering Albedo	*SSA*
High AOD-Low T_{air}	*HALT*
High AOD-High T_{air}	*HAHT*
Low AOD- High T_{air}	*LAHT*
Outgoing long wave radiation at surface	LW_{out}
canopy resistance	r_s
aerodynamic resistance to heat transfer	r_a
Sensible heat fraction	*SHF*
Latent heat fraction	*LHF*

* The overall quality of the figures is too poor for publication. Please make sure all figures have a consistent font size, are not stretched and have either a vector format, or a high enough resolution.

All Figures are replotted and extracted at finer resolutions for improvement in clarity.

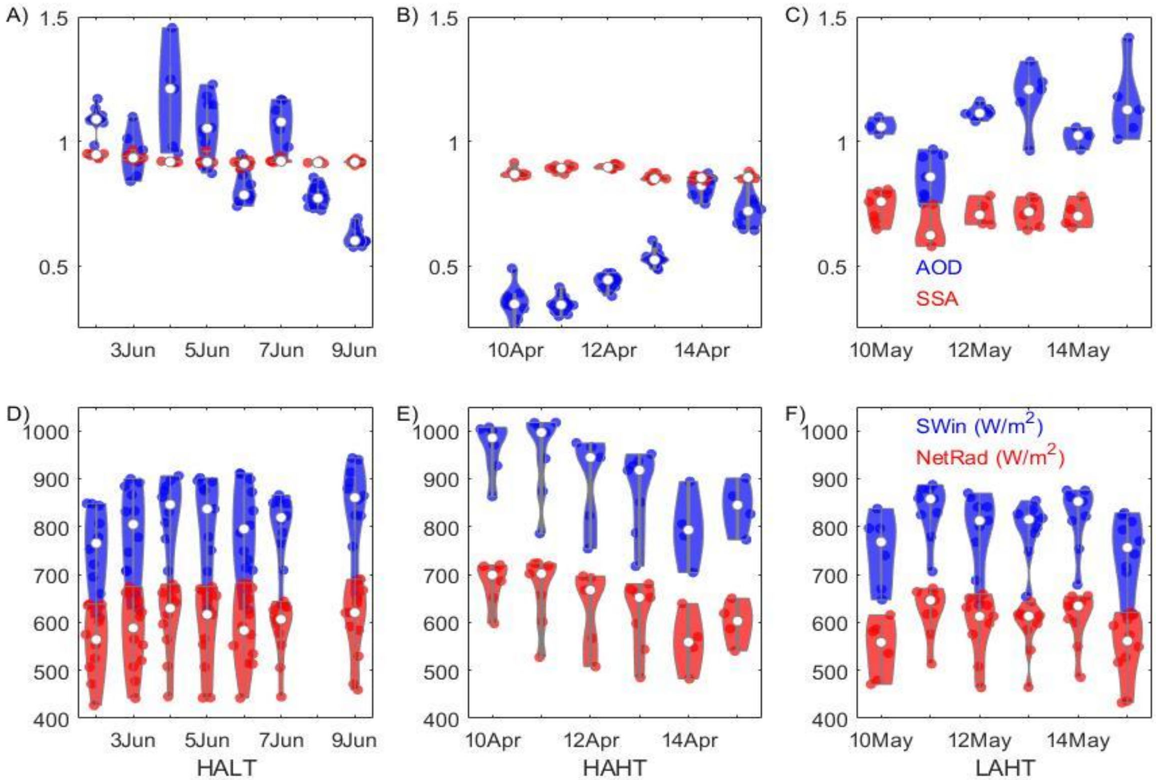

Figure 2: Distribution plots showing the variations in aerosol and radiation during the cases. Row 1 illustrates Time series of midday (1100-1400 LT) variation in AOD and SSA values during HALT, HAHT and LAHT, respectively.. The horizontal line within box represents median of the distribution. The bottom and top edge of the boxes represent 25th and 75th percentile, respectively, of the distribution. The short dash at top and bottom extent of the boxes represent 5th and 95th percentile, respectively. Row 2 is same as Row 1 but show measurements of incoming short wave radiation and net radiation at surface. Note that June,16 means June of 2016 and so on.

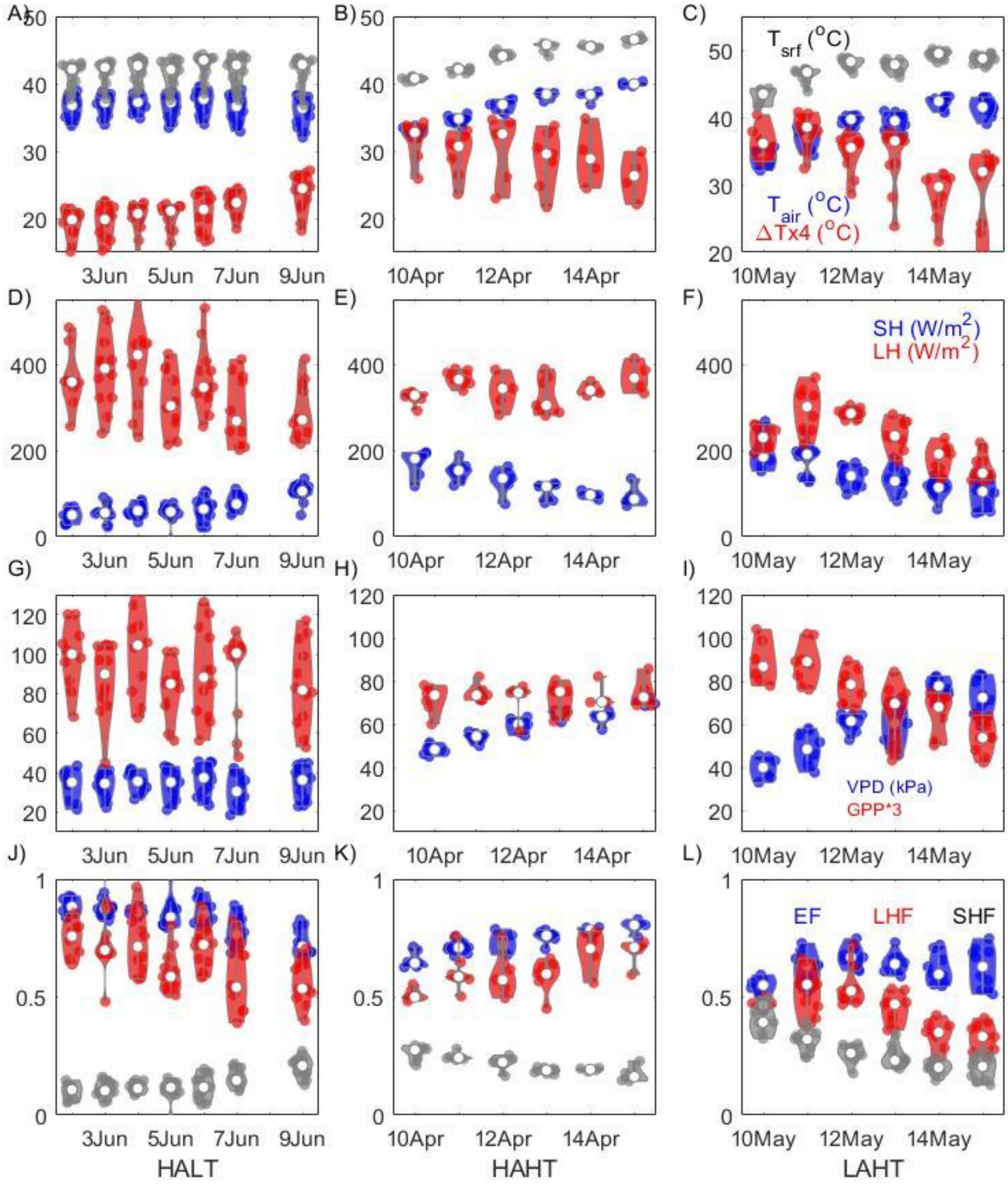

Figure 3: Distribution plots showing the variations in near surface meteorology and surface fluxes during the cases. Row 1 illustrates Time series of midday (1100-1400 LT) variation in T_{srf}, T_{air} and (-)ΔT values during HALT, HAHT and LAHT, respectively. Row 2 is same as Row 1 but for SH and LH. Row 3 is same but for VPD and GPP ; Row 4 is same but for EF, LHF (red) and SHF.

* Please use units consistently, I see W/m2 as well as W m^{-2}. Please add a space between different units.

Corrected.

* Line 71-73: the paper of Van Heerwaarden & Teuling (2014, Biogeosciences) shows exactly the threshold where VPD increase leads to a shutdown, rather than increase in ET.

We thank the reviewer for the reference. Please see our response to your main comment#1 above, where we have included relevant discussion on this point.

* Figure 4: Please check the units of VPD, these must be Pa for these values.

We have corrected this plot as below.

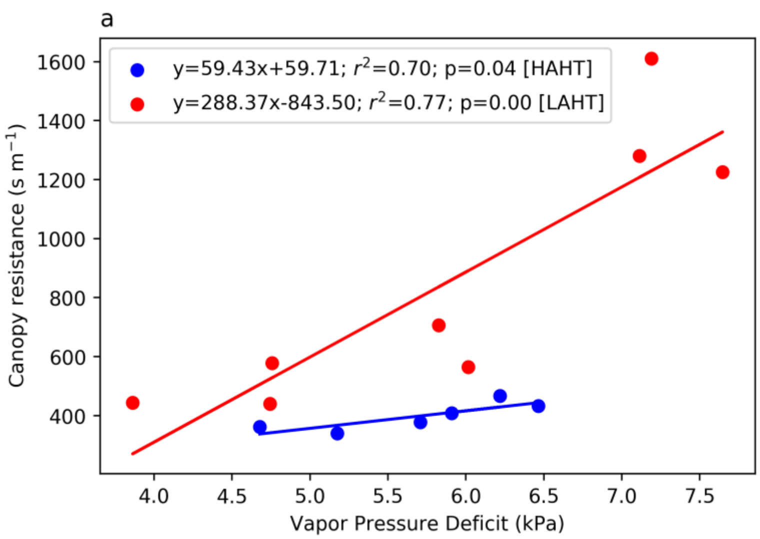

References:

1. Mwendia, S. W., Yunusa, I. A., Sindel, B. M., Whalley, R. D., & Kariuki, I. W. (2017). Assessment of Napier grass accessions in lowland and highland tropical environments of East Africa: water stress indices, water use and water use efficiency. *Journal of the Science of Food and Agriculture*, *97*(6), 1953-1961.
2. van Heerwaarden, C. C., & Teuling, A. J. (2014). Disentangling the response of forest and grassland energy exchange to heatwaves under idealized land–atmosphere coupling. *Biogeosciences*, *11*(21), 6159-6171.
3. Chakraborty, T., Sarangi, C., Krishnan, M., Tripathi, S. N., Morrison, R., & Evans, J. (2019). Biases in model-simulated surface energy fluxes during the Indian monsoon onset period. *Boundary-Layer Meteorology*, *170*(2), 323-348.
4. Juan Andrés Cardoso, Marcela Pineda, Juan de la Cruz Jiménez, Manuel Fernando Vergara, Idupulapati M. Rao, Contrasting strategies to cope with drought conditions by two tropical forage C_4grasses, *AoB PLANTS*, Volume 7, 2015, plv107, https://doi.org/10.1093/aobpla/plv107

5. Liang, X., Erickson, J.E., Sollenberger, L.E., Rowland, D.L., Silveira, M.L. and Vermerris, W. (2018), Growth and Transpiration Responses of Elephantgrass and Energycane to Soil Drying. Crop Science, 58: 354-363. https://doi.org/10.2135/cropsci2017.01.0019
6. Purbajanti, E.; Anwar, S.; Wydiati, F.K. Drought stress effect on morphology characters, water use efficiency, growth and yield of guinea and napier grasses. *Int. Res. J. Plant Sci.* 2012, *3*, 47. [Google Scholar]
7. Mwendia, S.; Yunusa, I.; Whalley, R.; Sindel, B.; Kenney, D.; Kariuki, I. Use of plant water relations to assess forage quality and growth for two cultivars of Napier grass (*Pennisetum purpureum*) subjected to different levels of soil water supply and temperature regimes. *Crop Pasture Sci.* 2014, *64*, 1008–1019. [Google Scholar]
8. Holm L, Pancho JV, Herberger JP, Plucknett DL, 1979. A Geographical Atlas of World Weeds. Toronto, Canada: John Wiley and Sons Inc
9. Charlotte Grossiord, Thomas N. Buckley, Lucas A. Cernusak, Kimberly A. Novick, Benjamin Poulter, Rolf T. W. Siegwolf, John S. Sperry, Nate G. McDowell
10. Irmak, S., and Mutiibwa, D. (2010), On the dynamics of canopy resistance: Generalized linear estimation and relationships with primary micrometeorological variables, *Water Resour. Res.*, 46, W08526, doi:10.1029/2009WR008484.